Seventh Framework Programme Theme 6 Environment

Collaborative Project (Large-scale Integrating Project)

Project no. **212085**

Project acronym: **MEECE**

Project title: **Marine Ecosystem Evolution in a Changing Environment**

D1.4 New model parameterisations

Part A: Acidification

Due date of deliverable: 31.08.2010
Actual submission date: 31.08.2011
Organisation name of lead contractor for this deliverable: UHAM

Start date of project: 01.09.08 Duration: 48 months
Project Coordinator: Icarus Allen, Plymouth Marine Laboratory

Project co-funded by the European Commission within the Seventh Framework Programme, Theme 6 Environment		
Dissemination Level		
PU	Public	x
PP	Restricted to other programme participants (including the Commission)	
RE	Restricted to a group specified by the consortium (including the Commission)	
CO	Confidential, only for members of the consortium (including the Commission)	

D1.4 Meta analysis of the driver databases and development of new parameterisations relevant to the ecosystem models

Part A: Acidification

New model parameterisations for ecosystem models to be developed in WP2

Acidification: (organisers UiB, NERC) will analyse data sets from T1.1 to develop parameterisations of ecosystem responses to acidification induced changes in stoichiometry, calcification, succession, primary production acidification experiments response experiments. A particular focus will be place on the results of large scale mesocosm experiments.

Contributors

UiB, NERC, PML

Contents

Meta Analysis: Enhanced phytoplankton carbon uptake under ocean acidification.

1. Introduction

A common response of marine phytoplankton to ocean acidification is an increase in the relative uptake of inorganic carbon to macronutrients resulting in an overconsumption of carbon by the ecosystem. As carbon is a major energy currency in the marine systems the channelling of extra carbon may result in significant perturbations to food web performance and marine biogeochemical cycling. The main aim of the phytoplankton meta-analysis was to 3 (Bellerby et al., 2008). Representations of carbon enhancement are often expressed as a function of the atmospheric CO2 representing results from deliberate perturbation experiments (e.g. Riebesell et al. 2007; MEECE deliverable D2.5)

$$C^{EN} = (pCO_2^{yr} - pCO_2^{2005}) * \alpha^{EN} + 1, \text{ where } \alpha^{EN} = 0.0005 \quad (1)$$

In these cases, there is no direct relationship to the ambient seawater carbon chemistry. Therefore, it was the objective of this work to relate observed changes in carbon and nutrient stoichiometry to the *in situ* carbonate chemistry. This was achieved through rigorous statistical analyses of new experimental data in close collaboration with MEECE modelling partners to develop process representations and parameterisations that can be incorporated and evaluated by MEECE models. For calcification, it is argued that there is no clear response to ocean acidification and therefore, no further analysis was performed (see Appendix II). Further, it was agreed at the MEECE workshop that it was not optimal to prescribe primary production and succession but that these processes should evolve in the models from a basal dependence of carbon to nutrient uptake on the ambient carbonate system influencing nutrient partitioning and plankton competition in the models. This is because most ecosystem approaches now simulate all the single processes and thus it is optimal to have as many free parameters as possible.

This analysis of the mesocosm experimental data assumes that the dominant processes were autotrophic and that bacterial respiration and zooplankton grazing were negligible. In this way NCP can represent new production and thus a carbon enhancement factor to ocean acidification can be directly related to the gross primary production. In an earlier MEECE workshop, and following further discussion with MEECE (ERSEM) modellers, it was agreed that a suitable approach would be to enhance the gross primary production according to:

$$m = m_{MAX} \times f(T) \times f(I, Chl, T) \times f(OA) \quad (2)$$

where μ_{MAX} is the maximum uptake rate (a constant value), f(T) describes the direct dependency of GPP on the Temperature, and f(I,Chl,T) describes the dependency of GPP on Light (I). The dependency on light is mediated by other variables too (Chl and T) and f(OA) describes how carbon uptake is influenced by ocean acidification.

2. Data source and data handling

We employed measurements from a mesocosm CO_2 perturbation experiment conducted in the Large-Scale Mesocosm Facility of the University of Bergen, Norway in 2005 (table 1), where the phytoplankton community was represented by a mixed assemblage, dominated by diatoms. Comprehensive information about the experimental set-up is found in Riebesell et al. (2008) and Schulz et al. (2008). The data were obtained from the MEECE deliverable D1.1, accessed through the MEECE website (for description of variables, see Appendix I), and further complimentary information about the EPOCA database is found in Nisumaa et al. (2010). We include calculations of daily net community production (NCP in µmol kg^{-1} day^{-1}); cumulative net community calcification (NCC or particulate inorganic carbon in µmol kg^{-1} day^{-1}); and net stoichiometric uptake ratios of carbon, nitrate and phosphate.

Table 1. Comprehensive information about the 2005 mesocosm experiment (based on published information)

Year	**2005**		
pCO_2 levels (ppmv)	1050	700	350
Time period	15.05.05 – 09.06.05		
Geometrical parameters	V – 25m^3, Depth – 9.5m, D – 2m		
Mixed layer depth	5.5m – fixed, airlift		
Nutrients addition	Day t-1		
Concentrations	NO_3 – 16 µmol/kg PO_4 – 0.8 µmol/kg		
Measured CO_2 system variables	DIC, AT and pCO_2		

3. Method

3.1 Calculations

Net community production (NCP) and net community calcification (NCC) were calculated according to Bellerby et al. (2008) and Delille et al. (2005):

$$TA_{corrected} = TA_{measured} - \Delta NO_3^- - \Delta H_2PO_4^- \quad (3)$$

$$NCC = -0.5 \times \frac{\Delta TA_{corrected}}{\Delta t} \quad (4)$$

$$NCP_{DIC} = -\frac{\Delta DIC}{\Delta t} + 0.5 \times \frac{\Delta TA_{corrected}}{\Delta t} \quad (5)$$

where $TA_{corrected}$ represents total alkalinity corrected for nutrient alkalinity changes. For more detail see MEECE deliverable D1.1.

3.2 Statistics

The statistical analysis is based on a subset (days 3 to 10) of the full dataset, representing the exponential bloom phase in the mesocosms.

The treatment pCO_2 (in ppmv) at the start of bloom were as follows:
High = 1050, Med = 700 and Low = 300.

For the first assumption, the potential of NCP at the beginning of each time step can be represented as a function of the standing stock of nutrients, autotrophic cell numbers (or dominant plankton functional type) and the seawater CO_2 chemistry (here represented by DIC).

$$dNCP_{x-y} \sim fn([PO4]_x, [Cells/Euk]_x, [DIC]_x \quad (6)$$

This can either be enforced as an **enhancement factor** or can be converted to cell specific carbon uptake rates.

$$\text{Specific carbon uptake} \sim fn\{([PO4]_x, [Cells/Euk]_x, [DIC]_x\}/[\text{cell count}_x] \quad (7)$$

Several correlation matrices were constructed in order to identify which variables were related in their evolution during the experiments and thus could be included as predictors (Table 2).

Table 2. Table showing the correlation matrix between daily change in NCP and other parameters in dataset in decreasing importance. See appendix 1 for variable names.

	All bags	High CO_2	Med CO_2	Low CO_2	mu	sd
NCP_d	100	100	100	100	100	0
HCO3_d	-99	-99	-99	-100	-99	0
TC_d	-96	-97	-98	-92	-96	3
Oar_d	93	95	96	92	94	2
CO3_d	91	95	92	89	92	2
fCO2_d	-87	-94	-95	-96	-93	4
CO2_d	-87	-94	-95	-96	-93	4
pCO2_d	-79	-85	-90	-83	-84	5
Ehux	72	67	79	73	73	5
NEuk2	62	60	64	64	62	2
CtoN_d	59	68	42	87	64	19
Bact	-54	-49	-65	-51	-55	7
Nit_d	-53	-48	-55	-68	-56	9
Chla	50	60	68	9	47	26
Oca_d	45	33	96	53	57	27
BacP_d	43	43	44	44	44	1
POP	42	42	47	36	42	4
Syn	-40	-34	-47	-43	-41	5
Peuk	-40	-57	-44	-15	-39	18
POP_d	39	23	44	56	40	14

NH4	-37	-30	-33	-53	-38	10
NEuk1	37	25	56	36	38	13
DOP	-36	-22	-56	-35	-37	14
DOC	-36	-35	-33	-48	-38	7
day	-35	-23	-35	-50	-36	11
T	-34	-24	-35	-48	-35	10
Nit	30	21	31	44	32	9
Si_d	-30	-19	-50	-16	-29	15
PO4_d	-26	-58	-27	-70	-45	22
POCP_d	25	21	31	26	26	4
DON	-24	-16	-19	-46	-26	14
S	23	24	20	29	24	4
PON_d	20	3	28	36	22	14
CtoP_d	19	43	8	77	37	31
PON	18	17	21	16	18	2
Syn_d	-17	-12	-15	-26	-18	6
Bact_d	15	15	19	11	15	3
pH_d	13	10	96	91	52	47
DOP_d	13	34	2	-8	10	18
Si	-12	-25	-11	5	-11	12

4. Results

Based on *a priori* knowledge of the model representation of planktonic systems and the information obtained from the correlation matrices (Table 2), statistical models were constructed with NCP as response, and phosphate (PO_4), total dissolved inorganic carbon (DIC), chlorophyll concentrations and total cell count as predictors. All the statistical models below are linear models (lm) of the form:

modelname <- lm (response ~ predictor1 + predictor2 +…+ predictorN) (8)

The results of the models are summarized in the coefficient table directly following each model. The first row shows the intercept of the regression line on the y-axis, and the slope for each of the predictors is detailed in the rows below. The two first columns represent the estimates for each parameter and the associated standard error, respectively. While the t-value and probability for the t-value, or the significance (at the 5% level), are given in the last two columns, respectively. Below the table we show the amount of total deviance explained (R^2) and the p-value (significance) of the model as a whole.

4.1 Model I

Here we predict daily NCP using a linear combination of phosphate, total inorganic carbon, the number of phytoplankton cells (cellcount) and the chlorophyll-*a* concentration:

mNCP <- lm (NCP_d ~ PO4 + DIC + cellcount + Chlorophyll) (9)

Coefficients:

	Estimate	Std. Error	t value	Pr(>|t|)	
(Intercept)	-1.114e+01	1.895e+01	-0.588	0.5587	
PO4	-1.099e+01	4.190e+00	-2.623	0.0108	*
TC	9.976e-03	9.986e-03	0.999	0.3214	
cellcount	1.340e-06	6.772e-07	1.978	0.0520	.
Chla	2.487e-01	1.436e-01	1.732	0.0878	.

R^2 = 0.41, p-value = 2.491e-07

The results of the mNCP model (9) are shown in figure 1. The measured daily NCP from the mesocosms is shown in the top panel, while the NCP predicted from the mNCP model is shown in the middle. The difference between the measured and predicted NCP is shown in the bottom panel. The model captures the general trend in the mesocoms with increased NCP in the medium and high CO_2 treatments (shown by symbols, see legend for explanation). The estimates for each parameter (as given in column 1 of the coefficient table) of the statistical model will then give the intercept of the regression line and the incremental slope of each of the predictor variables.

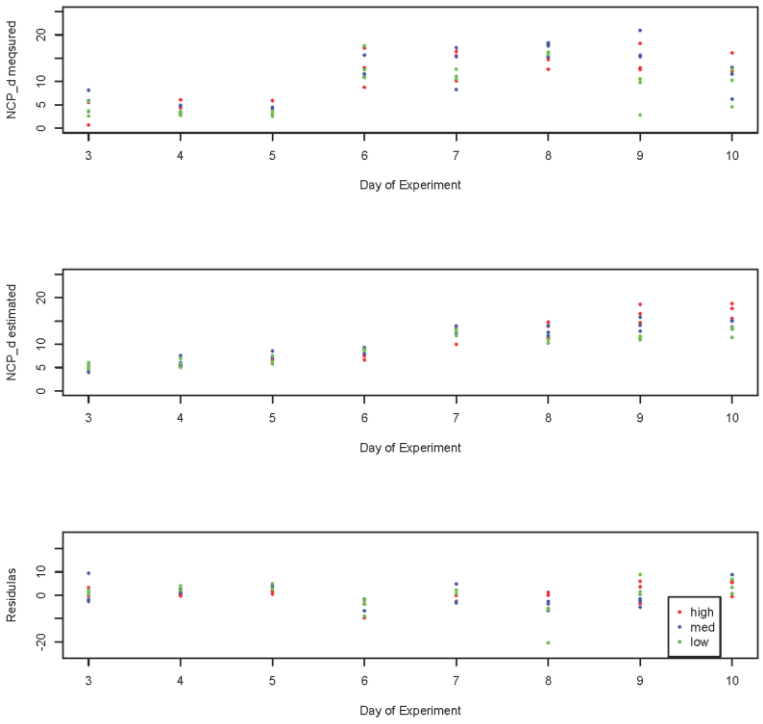

Figure. 1 Top plot shows daily NCP as calculated through (9), middle shows the daily NCP as estimated from mNCP (7), while the lower plot displays the residual between estimated and measured NCP.

Figure 2 shows NCP as estimated from mNCP against experimental nitrate uptake. We can see that there is higher NCP towards the end of the bloom in the high CO_2 treatment relative to the medium and low CO_2. In addition the high CO_2 treatment has a higher relative nitrate uptake.

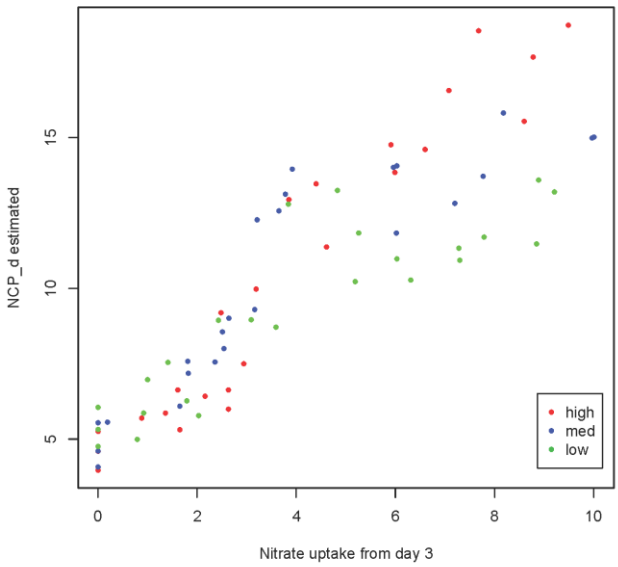

Figure.2 Plot showing estimated NCP through (7) against phytoplankton nitrate uptake relative to day 3.

Alternatively, the cell specific NCP (NCP_cell; NCP divided by cell count) can be used as the response variable, replacing cell count as a predictor in the model. This is more directly applicable to the processes being modelled in some ecosystem models like ERSEM. This statistical model was of the form:

mNCP_cell <- lm (NCP_cell ~ PO4 + DIC + Chlorophyll) (10)

Coefficients:

	Estimate	Std. Error	t value	Pr(>|t|)	
(Intercept)	2.752e-06	5.571e-07	4.940	3.81e-06	***
PO4_cell	-7.230e+00	1.838e+00	-3.933	0.000169	***
TC_cell	2.165e-03	8.106e-04	2.671	0.009052	**
Chla_cell	1.154e-01	1.034e-01	1.116	0.267386	

R^2 = 0.1547, p-value = 0.002262

As evident from the R^2, this model only describes 15% of the variation, compared to 41% when cell count is used as a predictor. This suggests that the simplified solution of dividing the NCP by cell count to get the cell specific NCP is not sufficient, hence a model of the form given in (9) is preferable.

Carbon enhancement factor

To be implemented in ecosystem models, the relationship from eq. (9) needs to be formulated as an enhancement factor. This can be achieved by relating it to a standard situation representing no

carbon enhancement. Here the latter is represented by a DIC value of 2000µmol kg^{-1}, being the DIC concentration in a typical winter situation in the area where the mesocosm study was conducted. The enhancement factor thus takes the form:

$$C^{en} = \frac{mNCP}{mNCP(DIC=2000)} = \frac{-11.14+10.99\times PO4+1.34E-6\times cell+0.2487\times Chl+.009976\times DIC}{-11.14+10.99\times PO4+1.34E-6\times cell+0.2487\times Chl+.009976\times 2000} = \frac{K+.009976\times DIC}{K+19.95} \quad (11)$$

where $K = -11.14+10.99*PO_4+1.34E^{-6}*cell+0.2487*Chl$ (12)

Implementing equations (11) and (12), into ecosystem models, follows straightforward from MEECE D2.5.

4.2 Model II

To create an enhancement factor for carbon to nutrient uptake shown under ocean acidification (figs 1 and 2), we need to relate the enhancement to a CO_2 concentration (DIC). In order to achieve do this we created regression models for each CO_2 treatment separately, where regressions models are fitted to a subset of the data for each treatment:

mNCP_high <- lm (NCP_d ~ PO4 + DIC + cellcount + Chla) (13)

mNCP_med <- lm (NCP_d ~ PO4 + DIC + cellcount + Chla) (14)

mNCP_low <- lm (NCP_d ~ PO4 + DIC + cellcount + Chla) (15)

The results of the regression models for each CO_2 treatment (ie. mNCP_low, mNCP_med and mNCP_high above) is shown in Fig. 3. The predicted NCP is shown versus experimental day, and there is a higher NCP in the high and medium CO_2 treatments relative to the low CO_2 treatment towards the end of the bloom.

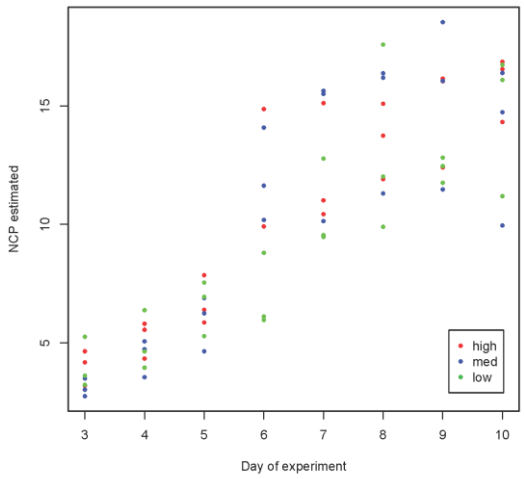

Figure. 3 NCP estimated for treatments separately vs Day

To investigate how the estimated NCP is related to for example nitrate uptake since the start of the bloom, we created a new linear model with the predicted NCP values for each treatment as response and relative nitrate uptake since the start of the bloom as predictor:

high_nit <- lm (predicted (mNCP_high) ~ Nit_rel (16)

med_nit <- lm (predicted (mNCP_med) ~ Nit_rel (17)

low_nit <- lm (predicted (mNCP_low) ~ Nit_rel (18)

The results are shown in Fig 4, which shows the same general response with increased nitrate uptake in the high and medium CO_2 treatments relative to the low CO_2 treatment. The parameter estimates for intercept and slopes, respectively, for each CO_2 treatments were as follows:

high_nit (5.198, 1.336)
(19)

med_nit (5.574, 1.217)
(20)

low_nit (4.885, 1.051)
(21)

To be implemented in ecosystem models, the **enhancement factor** would thus be represented by eq. (19) relative to eq. (21), i.e. the prediction from (16) divided by the one from (18). However as it is difficult evaluating what nitrate concentration is representative for the onset of the bloom, this approach is thus not optimal for ecosystem model implementation.

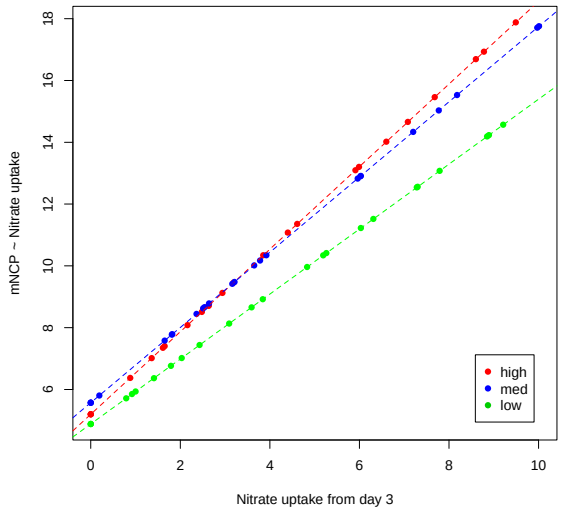

Figure. 4 NCP estimated for treatments separately vs Nitrate uptake

4.3 Model III

Here we employ an extended Multiple Linear Regression (eMLR) in order to construct the enhancement factor. Such an approach has previously been used for quantifying increasing anthropogenic CO_2 between two datasets (e.g. Friis et al., 2005, Hauck et al., 2010). The theory is that we can estimate the change in NCP daily (µmol kg^{-1} d^{-1}) between the low and high CO_2 treatments, which would then represent the relative enhanced C uptake caused by increasing DIC. This method would provide an equation for the difference between low and high CO_2 ($NCP_{enhance}$ below). Firstly linear regression models were fitted to the data for the low and high CO_2 treatments, respectively:

mNCP_low <- lm (NCP_d ~ PO4 + TC + cellcount + Chla) (22)

Coefficients:

	Estimate	Std. Error	t value	Pr(>|t|)
(Intercept)	-5.237e+02	3.497e+02	-1.498	0.1507
PO4	-4.679e+01	2.636e+01	-1.775	0.0919 .
TC	2.850e-01	1.860e-01	1.532	0.1419
cellcount	6.304e-08	1.510e-06	0.042	0.9671
Chla	-1.101e-02	6.131e-01	-0.018	0.9859

R^2: 0.377, p-value: 0.05116

mNCP_high <- lm (NCP_d ~ PO4_d + TC_d + cellcount_d + Chla_d) (23)

Coefficients:

	Estimate	Std. Error	t value	Pr(>|t|)
(Intercept)	1.107e+01	3.646e+02	0.030	0.9761
PO4	1.339e+01	1.709e+01	0.784	0.4428
TC	-9.213e-03	1.759e-01	-0.052	0.9588
cellcount	1.859e-06	1.312e-06	1.417	0.1727
Chla	1.097e+00	5.503e-01	1.994	0.0607 .

R^2: 0.6681, p-value: 0.0002069

A summary of the parameter estimates for the intercept and each predictor for the low and high CO_2 treatments is shown in Table 3.

Table 3. Summary of parameter estimates.

Coefficient	Variable	Low CO_2 treat (~300 ppm)	High CO_2 treat (~1000ppm)
B_0		-5.237e+02	1.107e+01
b_1	PO_4	-4.679e+01	1.339e+01
b_2	DIC	2.850e-01	-9.213e-03
b_3	Cellcount	6.304e-08	1.859e-06
b_4	Chla	-1.101e-02	1.097e+00
R^2		0.377	0.6681
Residual standard error		5.941	3.378
n		19	19

The equation for the difference between NCP in the low and high treatment can thus be calculated as:

NCP_{diff} = -534.77 + -60.18 PO4 + 0.294213 TC + -1.79596e-06 cell count + -1.10801 Chla (24)

With the **relative enhancement factor** of the form:

$$C^{en} = NCP_{diff} / NCP_{low}$$, where NCP_{low} is given in table 3.

(25)

If the estimated NCP for low and high CO_2 treatments is plotted against day (Fig. 5), we see that a higher NCP is predicted towards the end of the bloom for the high CO_2. The models therefore seem to reproduce the carbon enhancement found in the mesocosm experiments. However the R^2 and p-value for the low CO_2 treatment suggests that the linear model for this subset of data is only marginally significant, and fitting a statistical model to whole dataset (i.e. model 1) might be more robust.

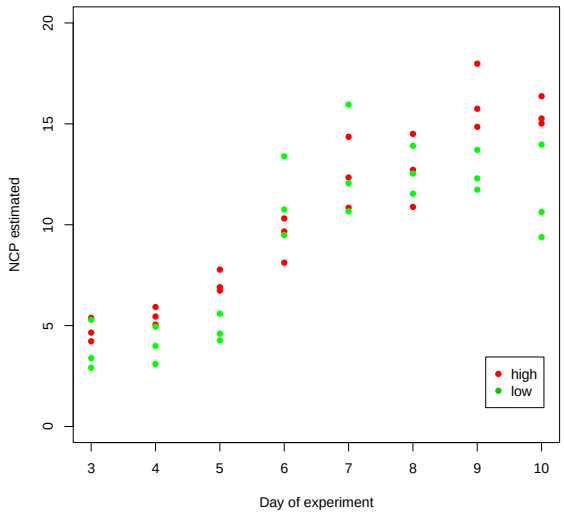

Figure. 5 NCP estimated for treatments separately vs Nitrate uptake

5. Summary and conclusions

The phytoplankton uptake stoichiometry carbon enhancement factor, as employed in D2.5, was dependant on the atmospheric pCO_2 relative to 2005. Through the phytoplankton meta-analysis we

have taken this approach a step forward and created alternative formulations informed by seawater carbon chemistry and phytoplankton bloom conditions. This approach is more realistic regarding biogeochemical and physiological conditions experienced in the real bloom situations in the ocean. The present parameterisations can be readily implemented in ecosystem models either as full ecosystem uptake response or as individual plankton functional type representation dependant on the model setup. The method can also easily be updated once more data becomes available from on-going and future ocean acidification experimentation.

6. References

Friis, K., A. Koertzinger, J. Pätsch & D.W.R. Wallace, 2005. On the temporal increase of anthropogenic CO2 in the subpolar North Atlantic. Deep-Sea Res. I 52:681-698; doi:10.1016/j.dsr.2004.11.017.

Hauck, J., Hoppema, M., Bellerby, R.G.J., Völker, C., Wolf-Gladrow, D.(2010). Data-based estimation of anthropogenic carbon and acidification in the Weddell Sea on a decadal timescale, Journal of Geophysical Research - Oceans, 115, C03004. doi:10.1029/2009JC005479

Bellerby, R. G. J., Schulz. K. G., Riebesell, U., Neil, C., Nondal, G., Johannessen, T., and Brown, K. R.: Marine ecosystem community carbon and nutrient uptake stoichiometry under varying ocean acidification during the PeECE III experiment. Biogeosciences, 5, 1517–1527, 2008.

Delille, B., Harley, J., Zondervan, I., Jacquet, S., Chou, L., Wollast, R., Bellerby, R.

G. J., Frankignoulle, M., Borges, A. V., Riebesell, U., and Gattuso, J. P.: Re25

sponse of primary production and calcification to changes of pCO2 during experimental

blooms of the coccolithophorid Emiliania huxleyi, Global Biogeochem. Cy., 19, GB2023,

doi:10.1029/2004GB002318, 2005.

Nisumaa A.-M., Pesant S., Bellerby R. G. J., Delille B., Middelburg J., Orr J. C., Riebesell U., Tyrrell T., Wolf-Gladrow D. & Gattuso J.-P., 2010. EPOCA/EUR-OCEANS data compilation on the biological and biogeochemical responses to ocean acidification. *Earth System Science Data* 2:167-175

Riebesell, U. Bellerby, R., Grossart, H.-P., Thingstad, F. (2008) Mesocosm CO2 perturbation studies: from organism to community level. *Biogeosciences* 5, 1157-1164

Schulz, K.G., Riebesell, U., Bellerby, R.G.J., Biswas, H., Meyerhöfer, M., Müller, M.N., Egge, J.K., Nejstgaard, J.C., Neill, C., Wohlers, J., Zöllner, E. (2008) Build-up and decline of organic matter during PeECE III. *Biogeosciences* 5, 707-718

Appendix I. Description of the PeECE III (2005) EPOCA dataset

No	Variable	Description
1	bag	bag number
2	day	experimental day
3	S	salinity
4	T	temperature
5	pH	pH
6	CO2	CO2 aqueous
7	pCO2	partial pressure of CO2
8	fCO2	fugacity of CO2
9	HCO3	bicarbonate ion
10	CO3	carbonate ion
11	TC	total inorganic carbon
12	TA	total alkalinity
13	Oar	saturation state of aragonite
14	Oca	saturation state of calcite
15	DOC	dissolves organic carbon
16	DON	dissolved organic nitrogen
17	DOP	dissolved organic phosphorus
18	POP	particulate organic phosphorus
19	PON	particulate organic nitrogen
20	POC/PON	CN ration of organic matter
21	Nitrate_ite	nitrate and nitrite
22	NH4	ammonia
23	PO4	phosphate
24	Si	silicate
25	Chla	chlorophyll a total
26	Synech	Synechococcus cells number
27	Peuk	PicoEucariotes cells number
28	Ehux	Emiliania huxley
29	NEuk1	Nanoeucariotes group 1
30	NEuk2	Nanoeucariotes group 2
31	Bact	Bacteria cells number (total)
32	BactProd	Bacteria production (leucine incorporation)
33	S_d	Daily change in Salinity ($t_n - t_{n-1}$)
34	T_d	Column 34 – 64 as above
35	pH_d	
36	CO2_d	
37	pCO2_d	
38	fCO2_d	
39	HCO3_d	
40	CO3_d	
41	TC_d	
42	TA_d	
43	Oar_d	
44	Oca_d	
45	DOC_d	
46	DON_d	
47	DOP_d	
48	POP_d	

49	PON_d	
50	POC/PON_d	
51	Nitrate_ite_d	
52	NH4_d	
53	PO4_d	
54	Si_d	
55	Chla_d	
56	Synech_d	
57	Peuk_d	
58	Ehux_d	
59	NEuk1_d	
60	NEuk2_d	
61	Bact_d	
62	BactProd_d	
63	NCC_d	Net community calcification (NCC)
64	NCP_d	Net community production (NCP)
65	CtoN_d	C:N ratio (NCP/N_d)
66	CtoP_d	C:P ratio (NCP/P_d)
67	NtoP_d	N:P ratio (N_d/P_d)
68	I	Irradiance
69	I_d	Irradiance daily change

Colour codes:
Nutrients: inorganic, organic particulate and dissolved
Biology: phytoplankton and bacteria cells
Carbon system: CO2 system
Physical environment: temperature and salinity, light intensity in the water (PAR)

NCC, NCP, C:N ratio, C:N ratio, N:P ratio are not present in ‘absolute concentrations’, because these variables are calculated as rates, shown here as daily changes.

Appendix II

Lack of Sensitivity of Coccolithophore Calcification to Ocean Acidification.

There have been a large number of studies looking into the effects of ocean acidification on coccolithophore calcification. Results are rather contradictory and ambiguous. Although there are more experimental studies pointing to lower than higher calcification at high CO_2 and low pH (low $CaCO_3$ saturation), there is great variability and a lack of a strong consensus. Moreover, observational studies (present-day ocean and paleoceanographic) are also both equivocal in terms of effects of OA on coccolithophore calcification.

Culture and Mesocosm Experiments.

Along with other calcifiers, coccolithophores such as *Emiliania huxleyi* are potentially susceptible to ocean acidification (OA) because of a possible impact on their ability to calcify. A large number of experimental studies *(e.g. 1-11)* have investigated this possibility. An early study *(1)* supported susceptibility (Figure A1a), as have a considerable number of subsequent experiments. There have also, however, been a number of studies obtaining divergent results, including one in particular *(7)* that found increasing calcification at high CO_2 (Figure A1b). It has been shown *(11)* that different species exhibit different responses to varying CO_2. It has even been found *(10)* that different strains of the same species (*Emiliania huxleyi*), exhibit different responses. Considering just *E. huxleyi* (the most common coccolithophore), many experiments have found depressed calcification at elevated CO_2 concentration and the associated low pH and low $CaCO_3$ saturation state (Ω) *(1-6)*, whereas others have found elevated calcification *(7-9)* or no trend (*9*). Four different strains of *E. huxleyi* cultured under identical environmental conditions exhibited varying responses to elevated CO_2 (*10*). New results continue to be reported in the literature, some showing reduced calcification at high CO_2, some not. Overall, diverse calcification responses have been reported from culture and mesocosm experiments (*1-11*).

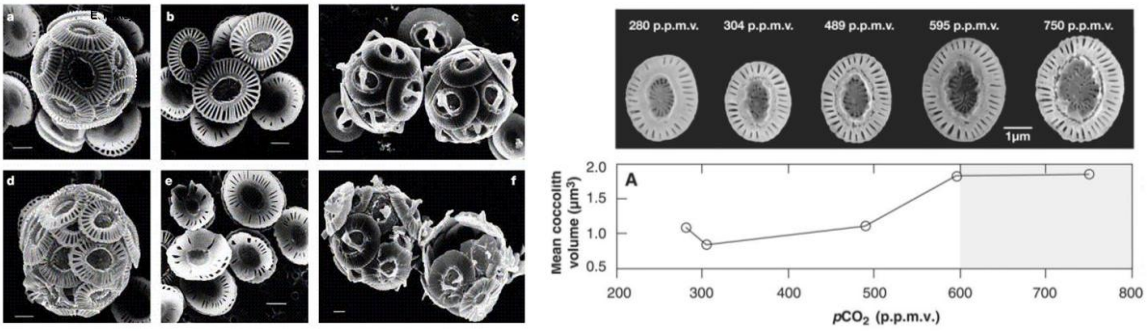

Figure A1. Variable Responses in two culture experiments. One experiment (left) found less calcification and malformed coccoliths at high CO_2 (bottom row of images) (1), whereas another (right) found greater calcification and larger coccoliths at high CO_2 (7).
Results were summarised by Andy Ridgwell and colleagues (11), as shown in Table A1. On the basis that calcification does not seem to be uniformly impacted across species and strains, they concluded with the prediction that, while calcification may not be depressed in all species, acidification will produce: "a transition in dominance from more to less heavily calcified coccolithophores"(11).

Table 1. Synthesis of available coccolithophorid calcification carbonate chemistry manipulation experiments.

Species	Strain (Clone)	Isolation date and location	Experimental design	Ambient light environment [1]	Carbonate chemistry manipulation	Calcification response [2]	Calcification response [3]	$CaCO_3$/POC response [10]	Reference [11]
Emiliania huxleyi	NZEH (CAWPO6)	1992 South Pacific	laboratory culture	12:12 h L:D 150 μmol m^{-2} s^{-1}	CO_2 bubbling	↑	↑	↔	*1*
Emiliania huxleyi	MBA 61/12/4	1991 North Atlantic	laboratory culture	12:12 h L:D 150 μmol m^{-2} s^{-1}	CO_2 bubbling	↑	↑	n/a	*1*
Emiliania huxleyi	PML B92/11A	1992 North Sea	laboratory culture	18:6 h L:D 150 μmol m^{-2} s^{-1}	acid/base	n/a	↓	↓	*2,5*
Emiliania huxleyi	PML B92/11A	1992 North Sea	laboratory culture	24:0 h L:D 150 μmol m^{-2} s^{-1}	acid/base	n/a	↓	↓	*2,5*
Emiliania huxleyi	CCMP 371	1987 Sargasso Sea	laboratory culture	12:12 h L:D 50 μmol m^{-2} s^{-1}	CO_2 bubbling	↔	n/a	↓	*3*
Emiliania huxleyi	CCMP 371	1987 Sargasso Sea	laboratory culture	12:12 h L:D 400 μmol m^{-2} s^{-1}	CO_2 bubbling	↓	n/a	↓	*3*
Emiliania huxleyi	TW1	2001 W Mediterranean	laboratory culture	24:0 h L:D 570 μmol m^{-2} s^{-1}	CO_2 bubbling	↓	↓	↔	*4*
Emiliania huxleyi	88E	1988 Gulf of Maine	laboratory culture	24:0 h L:D 50 μmol m^{-2} s^{-1}	acid/base	n/a	↔ [4]	↔ [4]	*9*
Emiliania huxleyi	Ch 24-90	1991 North Sea	laboratory culture	16:8 h L:D 300 μmol m^{-2} s^{-1}	CO_2 bubbling	n/a	↔ [5]	↔ [5]	*10*
Emiliania huxleyi	NZEH (PLY M219)	1992 South Pacific	laboratory culture	24:0 h L:D 150 μmol m^{-2} s^{-1}	acid/base	↑	↑	↔	*11*
Gephyrocapsa oceanica	PC7/1	1998 Portuguese shelf	laboratory culture	18:6 h L:D 150 μmol m^{-2} s^{-1}	acid/base	n/a	↓	↓	*2,5*
Calcidiscus leptoporus	AC365	2000 South Atlantic	laboratory culture	16:8 h L:D 350 μmol m^{-2} s^{-1}	acid/base	n/a	↓ [6]	↓ [6]	*6*
Coccolithus pelagicus	AC400	2000 South Atlantic	laboratory culture	16:8 h L:D 350 μmol m^{-2} s^{-1}	acid/base	n/a	↔	↔	*6*
Emiliania huxleyi [7]	n/a	n/a (North Sea)	mesocosm [8]	95% of ambient surface irradiance	CO_2 bubbling	n/a	↓ [9]	↓ [9]	*7,8*
subarctic North Pacific natural assemblages	n/a	n/a (N. Pacific)	ship-board incubation	30% of ambient surface irradiance	CO_2 bubbling	n/a	↓ [9]	↓ [9]	*2*
subarctic North Pacific natural assemblages	n/a	n/a (N. Pacific)	ship-board incubation	30% of ambient surface irradiance	acid/base	n/a	↓ [9]	↓ [9]	*2*

Table A1. Summary of Variable Responses. Table summarising results across a number of experimental studies *(taken from 12)*. A red arrow shows reduced calcification at higher CO_2, a blue arrow the reverse, a green arrow no effect.

Lack of Evidence of a Future Assemblage Shift to Less Calcified Forms.

While there is some support for this view from in-situ studies, the evidence is, however, again very equivocal. Laboratory studies are unrealistic in many respects and, because of their typically short timescales, preclude the possibility of evolutionary adaptation to the imposed change, a key uncertainty in OA research *(11)*. Another weakness is that the cultured organisms were often isolated from the ocean many decades ago, and hence could be considered to be evolved to fit laboratory rather than natural conditions.

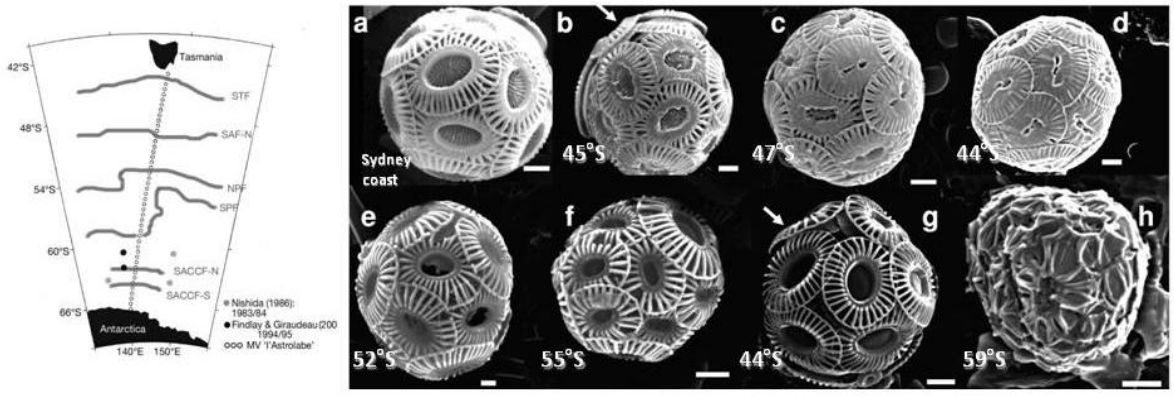

Figure A2. Variable Coccolith Morphology in the Ocean. Sampling of surface water along a transect (left) found considerable variability in coccolith appearance (right) (13).

It is therefore vital to complement laboratory experiments with observational studies of coccolithophores living in the natural habitats to which they are evolutionarily adapted. Observational work from the Southern Ocean *(13)* (figure A2) supports the supposition of reduced calcification at high CO2 (low Ω; it gets lower further south in the Southern Ocean, and coccoliths simultaneously become more fragile). Many other environmental factors, most obviously temperature, also change with latitude in the Southern Ocean, however, and so coccolith morphology changes cannot be securely attributed to changes in Ω. Moreover, other observational evidence argues against a strong control by Ω. Samples collected every month over two years, between UK and Spain *(14)*, revealed a pronounced seasonality in *Emiliania huxleyi* morphology in the Bay of Biscay. An inverse correlation was found between Ω and degree of coccolith calcification. More heavily calcified forms were found to be more abundant when Ω was low, not when it was high. Whereas pH and $CaCO_3$ saturation are highest in summer, the population shifts from <10 (summer) to >90% heavily calcified (winter), contrary to the supposition that more heavily calcified coccolithophores will be selected against in future *(14)*.

Geological evidence is also equivocal with regards to the proposition that, as seawater becomes more acidic, competition between more heavily and more lightly calcified forms will result in a shift in ecotype towards the latter. It has been suggested (*15*) that heavily calcified forms strongly declined in abundance during a Cretaceous acidification event. However, this suggestion is controversial (*16).* The occurrence of (a) acidification, and (b) a shift in degree of calcification, are both contested *(16)*.

Appendix references

1 U. Riebesell et al., Reduced calcification of marine plankton in response to increased atmospheric CO2. Nature **407**, 364-367 (2000).

2 I. Zondervan, B. Rost, U. Riebesell, Effect of CO2 concentration on the PIC/POC ratio in the coccolithophore Emiliania huxleyi grown under light-limiting conditions and different daylengths. J Exp Mar Biol Ecol **272**, 55-70, doi:Pii S0022-0981(02)00037-0 (2002).

3 B. Delille, et al., Response of primary production and calcification to changes of pCO(2) during experimental blooms of the coccolithophorid Emiliania huxleyi. Global Biogeochem Cy **19**, GB2023, doi:10.1029/2004gb002318 (2005).

4 A. Engel, et al., Testing the direct effect of CO2 concentration on a bloom of the coccolithophorids Emiliania huxleyi in mesocosm experiments. Limnol Oceanogr **50**, 493 - 507 (2005).

5 A. Sciandra, et al., Response of coccolithophorid Emiliania huxleyi to elevated partial pressure of CO2 under nitrogen limitation. Mar Ecol-Prog Ser **261**, 111-122 (2003).

6 Y. Feng, et al., Interactive effects of increased pCO2, temperature and irradiance on the marine coccolithophore Emiliania huxleyi (Prymnesiophyceae). Eur J Phycol **43**, 87 – 98, doi:10.1080/09670260701664674 (2008).

7 M. D. Iglesias-Rodriguez et al., Phytoplankton calcification in a high-CO2 world. Science **320**, 336-340, doi:10.1126/science.1154122 (2008).

8 D. Shi, Y. Xu, F. M. M. Morel, Effects of the pH/pCO(2) control method on medium chemistry and phytoplankton growth. Biogeosciences **6**, 1199-1207 (2009).

9 B. E. Casareto, M. P. Niraula, H. Fujimura, Y. Suzuki, Effects of carbon dioxide on the coccolithophorid Pleurochrysis carterae in incubation experiments. Aquat Biol **7**, 59-70, doi:10.3354/Ab00182 (2009).

10 G. Langer, G. Nehrke, I. Probert, J. Ly, P. Ziveri, Strain-specific responses of Emiliania huxleyi to changing seawater carbonate chemistry. Biogeosciences **6**, 2637-2646 (2009).

11 G. Langer et al., Species-specific responses of calcifying algae to changing seawater carbonate chemistry. Geochem Geophy Geosy **7**, Q09006, doi:10.1029/2005gc001227 (2006).

12 A. Ridgwell et al., From laboratory manipulations to Earth system models: scaling calcification impacts of ocean acidification. Biogeosciences **6**, 2611-2623 (2009).

13 J. C. Cubillos, et al., Calcification morphotypes of the coccolithophorid Emiliania huxleyi in the Southern Ocean: changes in 2001 to 2006 compared to historical data. Mar Ecol-Prog Ser **348**, 47-54, doi:10.3354/Meps07058 (2007).

14 Helen E.K. Smith, Toby Tyrrell, Anastasia Charalampopoulou, Cynthia Dumousseaud, Oliver J. Legge, Sarah Birchenough, Laura R. Pettit, Rebecca Garley, Sue E. Hartman, Mark C. Hartman, Navjit Sagoo, Eric P. Achterberg & David J. Hydes. Overcalcified Coccolithophores at Low $CaCO_3$ Saturation during Winter in the Bay of Biscay. Submitted.

15 E. Erba, C. Bottini, H. J. Weissert, C. E. Keller, Calcareous Nannoplankton Response to Surface-Water Acidification Around Oceanic Anoxic Event 1a. Science **329,** 428-432 (2010).

16 S. J. Gibbs, et al. "Comment on, Calcareous Nannoplankton Response to Surface-Water Acidification Around Oceanic Anoxic Event 1a. Science **332,** 175 (2011).